Active Log-Periodic Dipole Antenna with Integrated Power Amplifier–Coupler for S-Band Duplex Operation

Chaabani Ala Eddine[1,2], Mejri Fethi[1] and Tijeni Delleji[2]

***Abstract*—This work presents a planar active log-periodic dipole antenna (LPDA) fed by an optimized 50 Ω microstrip line for S-band applications. The proposed antenna replaces the conventional coaxial feeding structure with a compact planar microstrip configuration, leading to reduced feeder losses and improved integration capability.**

To experimentally evaluate the antenna under realistic transmission and reception conditions, an active front-end composed of a Mini-Circuits GALI-84+ power amplifier and a 3 dB/90° hybrid coupler is integrated into the measurement architecture. The hybrid coupler ensures signal separation and isolation between the transmission and reception paths.

The proposed antenna performance is analyzed through scattering parameters and radiation characteristics. A good agreement between simulated and measured results validates the proposed design and demonstrates stable wideband operation suitable for RADAR applications.

I. INTRODUCTION

The fast evolution of communication technologies over the past decade has significantly increased the demand for efficient and versatile antennas capable of supporting a wide range of applications . Nowadays, antennas play a crucial role in ensuring reliable wireless communication, where performance, bandwidth, and polarization characteristics are key design factors [1].

The log periodic dipole antenna (LPDA), known for its inherent wideband operation and stable radiation characteristics, is widely used in modern wireless communication systems. Typical applications include broadband and IoT networks, 5G systems, radio direction-finding, airborne platforms, radar systems, mobile imaging, digital television reception, and electromagnetic compatibility measurements [2].

LPDAs achieve wideband performance by arranging dipole elements in a logarithmic progression, where the length and spacing of each element scale proportionally with the logarithm of the operating frequency [3].

Although several LPDA structures have been reported in the literature for broadband wireless applications, many existing designs still suffer from limitations such as large physical dimensions, complex feeding structures, limited gain stability, or the absence of integrated duplexing functionality [3].

Moreover, conventional LPDA systems generally rely on external duplexers and coaxial feeding structures, which increase system complexity and insertion losses. Therefore, there is still a need for compact and efficient LPDA configurations capable of integrating active circuitry and duplexing functions within a simplified RF front-end.

This paper proposes an original active LPDA configuration based on a newly designed 50 Ω microstrip feed line that replaces the conventional coaxial cable. Unlike traditional approaches employing a dedicated duplexer, the proposed configuration uses a hybrid coupler combined with a power amplifier to implement the duplexing functionality. This technique simplifies the RF front-end while maintaining adequate isolation between the transmission and reception paths.

In transmission systems where one antenna is used for transmission and reception, a duplexer is required to separate the transmitted and received signals and to ensure sufficient isolation between the two paths. In this work, the duplexing function is implemented using a hybrid coupler, which serves as the main component for signal routing and isolation between the Tx and Rx channels [4].

A close agreement between experimental and simulated results validates the presented antenna design. Moreover, the antenna configuration and design methodology provide good impedance matching and stable gain across the operating band [5], [6].

II. ANTENNA DESIGN

This work presents a planar, active log-periodic dipole antenna (LPDA) operating over the 2.3–2.5 GHz frequency band. The design includes a printed LPDA, a 50 Ω microstrip feed line, a PA and a coupler. The entire structure is made using standard printed circuit board (PCB) made of Flame Retardant 4 (FR4) substrate, chosen for its low cost and adequate radio-frequency performance in printed antenna applications [7]. The conductor is copper with a thickness of 0.035 mm and conductivity of 5.96×10^7 S/m. The substrates have a thickness of 1.5 mm, a relative permittivity (ε_r) of 4.32 and dielectric loss tangent (tan δ) of 0.02.

A. LPDA

Originally invented in the 1950s by Dwight E. Isbell and Raymond DuHamel, the log-periodic dipole antenna was originally proposed by the University of Illinois at Urbana-Champaign and has since become a key component for several applications [8]–[10].

The development of an LPDA relies on fundamental relationships between the antenna elements' lengths and spacings, governed primarily by the scaling factor τ and the spacing factor σ. These parameters enable the antenna to achieve its broadband characteristics by ensuring the elements scale logarithmically along the array. The following formulas detail how

[1]Sys'Com Research Laboratory, National Engineering School of Tunis (ENIT), Le Bélvédère, El Manar, 1002, Tunis, Tunisia

[2]Science and Technology for Defense Lab (STD), Military Research Center, Taieb Mhiri, Aouina, 2045, Tunis, Tunisia

to compute the lengths and spacings of the dipole elements based on these factors [8]–[10].

The length of the dipoles is determined by:

$$L_{i+1} = L_i \times \tau \quad (1)$$

The lengths of the first and last dipoles, L_1 and L_N, are calculated using the following equations:

$$L_1 = \frac{c}{2 f_{\max} \sqrt{\varepsilon_r}} \quad (2)$$

$$L_N = \frac{c}{2 f_{\min} \sqrt{\varepsilon_r}} \quad (3)$$

where:

- $f_{\max}$ is the upper operating frequency,
- $f_{\min}$ is the lower operating frequency,

The width of each dipole is calculated by:

$$W_{i+1} = W_i \times \tau \quad (4)$$

The spacing between two successive dipoles :

$$S_{i+1} = S_i \times \tau \quad (5)$$

The Scaling Factor:

$$\tau = \frac{L_{i+1}}{L_i} = \frac{S_{i+1}}{S_i} \quad with \quad \tau < 1 \quad (6)$$

The Spacing Factor :

$$\sigma = \frac{S_1}{2 \times L_1} = \frac{S_n}{2 \times L_n} < 1 \quad (7)$$

The number of dipoles N is calculated as follows:

$$N = 1 + \frac{\log\left(\frac{f_{\max}}{f_{\min}}\right)}{\log\left(\frac{1}{\tau}\right)} \quad (8)$$

Following the original work on log-periodic antennas by Isbell and DuHamel, Carrel proposed an optimization approach to improve antenna design. Carrel's graph, illustrated in Fig. 1, is a fundamental tool for determining the dimensions of the LPDA. This graph features gain contour lines ranging from 6 to 10.5 dB, with the scaling factor τ arranged along the horizontal axis and the spacing factor σ along the vertical axis. Beyond the gain contours, the graph includes an optimum design curve that represents the best compromise among bandwidth, gain and input impedance characteristics. The intersections of this curve with the gain contours correspond to unique pairs of (τ, σ) values that achieve the desired gain while ensuring optimal antenna performance. During the design process, the target gain is first specified, after which the corresponding scaling and spacing factors are extracted from Carrel's graph [10]. These parameters are then used to calculate the physical dimensions of the LPDA antenna.

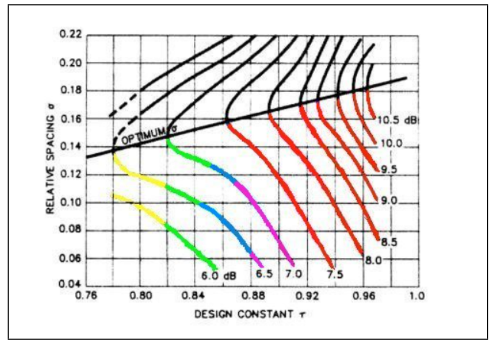

Fig. 1: Carrel's graph : Gain of LPDA as a function of τ and σ [10].

The antenna is designed and fabricated to operate over the 2.3–2.5 GHz frequency band with a target gain of 7 dB. Furthermore, using Carrel's graph in Fig. 1, the antenna parameters are determined as follows: the spacing factor $\sigma = 0.15$ and the scaling factor $\tau = 0.82$. After optimization, the number of elements obtained is $N = 8$ as depicted in Fig. 2.

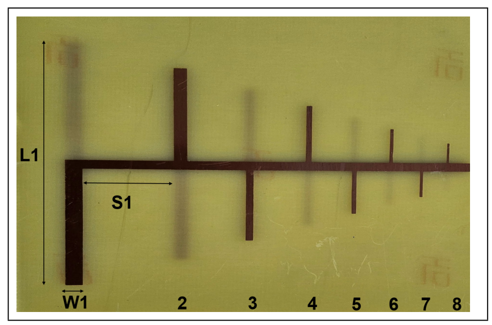

Fig. 2: the fabricated LPDA antenna.

As shown in Fig. 2, The LPDA radiating elements are implemented on both sides of the dielectric substrate. and the overall length of the antenna is 77.06 mm; however, an additional margin of 16.28 mm is intentionally left before the longest element to achive the quarter-wavelength ($\lambda/4$) requirement to install a reflector(if needed). This value corresponds to the guided wavelength on an FR4 substrate, calculated using its relative permittivity ε_r at the center frequency of 2.4 GHz.

B. Microstrip feed line 50 Ω

One of the important parameters in the design of the LPDAs is the feeding method, including the feed type and its location, as it plays an importing role in controlling impedance matching, gain and radiation characteristics [11].

Conventionally, LPDAs are fed using coaxial cables due to their simplicity of fabrication and the wide availability of standard connectors and cables. In usual configuration, the outer conductor of the coaxial cable is soldered to the bottom feed line, while the inner conductor is connected to the upper feed line through a hole in the substrate [7], [12].

In this study, the antenna is excited using a printed microstrip feed line implemented on an FR4 substrate, which simplifies manufacturing and integration. Various feeding techniques can be employed for LPDA antennas, depending on the desired performance and fabrication constraints.

Fig. 3 illustrates the proposed microstrip feed line, highlighting its three-layer structure: the bottom copper ground plane, the dielectric substrate and the top microstrip feed line.

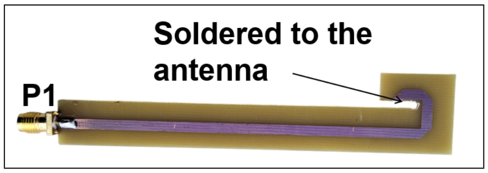

Fig. 3: The microstrip feed ligne

The microstrip feed line is extended by $\lambda/4$ relative to the antenna length and has a width of 2.89065 mm, ensuring a characteristic impedance of $50\,\Omega$. The total length of the feed line is 93.34 mm, which corresponds to the antenna length plus the additional $\lambda/4$ section.

III. The duplexer

A duplexer (Fig. 4) is an RF component that enables a single antenna to operate in both transmission and reception modes while ensuring proper impedance matching for each path. It is composed of three ports: a transmit (Tx) port, a receive (Rx) port, and a common antenna port (Tx/Rx). High isolation is maintained between the transmit and receive channels to prevent interference. In operation, the duplexer directs the transmitter signal to the antenna and routes the received signal from the antenna to the receiver, effectively acting as a bidirectional switching network [13].

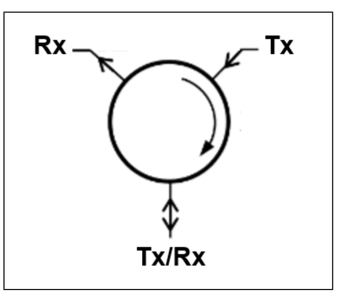

Fig. 4: Block diagram of the duplexer

The scattering matrix of the duplexer is defined as follows:

$$[S] = \begin{bmatrix} S_{11} & S_{12} & S_{13} \\ S_{21} & S_{22} & S_{23} \\ S_{31} & S_{32} & S_{33} \end{bmatrix} = \begin{bmatrix} 0 & 0 & 0 \\ 0 & 0 & 1 \\ 1 & 0 & 0 \end{bmatrix}$$

The conventional duplexer, as shown in Fig. 5, is composed of several components, including magnets and ferrites [14]. In this work, the duplexer will be magnetically biased by using a power amplifier and a 3 dB/90° hybrid coupler.

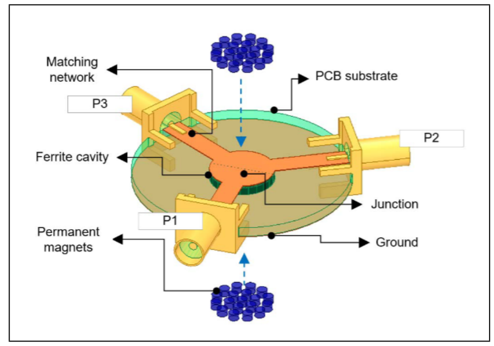

Fig. 5: Layout of microstrip circulator showing a permanent magnet that provides DC bias and a ferrite cylinder [14].

A. Amplifier

Power amplifiers are key components in RF design for wireless communication. They boost the input signal to the needed output power while keeping efficiency high and power consumption low [15].

In this work, we added an external RF power amplifier (PA) to strengthen the transmitted signal and reduce losses in the feeding network. The use of the amplifier increases the transmitted power and cuts down feeder losses, turning the antenna system into an active transmitter where the radiated power isn't limited by the source signal anymore.

The compact RF amplifier stage, shown in Fig. 6, is built on an FR4 board and uses the Mini-Circuits GALI-84+ MMIC [16]. Having the amplifier close to the antenna means the signal gets amplified early, which cuts feeder losses and improves overall efficiency.

Fig. 6(a) shows the block diagram of the GALI-84+-based power amplifier, taken straight from the datasheet [16]. Fig. 6(b) shows the fully assembled PCB with the GALI chip, resistors, two power cables for Vcc and two SMA connectors for RF input and output.

The amplifier runs on a 12 V DC supply delivered through a T-bias network that keeps the DC path separate from the RF signal. This 12 V level comes from a 61.9 kΩ bias resistor, chosen following the datasheet [16]. DC-blocking capacitors at the input and output stop DC from passing through while letting the RF signal flow cleanly.

The whole circuit is designed for a 50 Ω impedance, which ensures good matching between the RF source, amplifier, and antenna. This setup allows the GALI-84+ provide enough gain for low-power active antenna transmission, while staying stable over a wide frequency range.

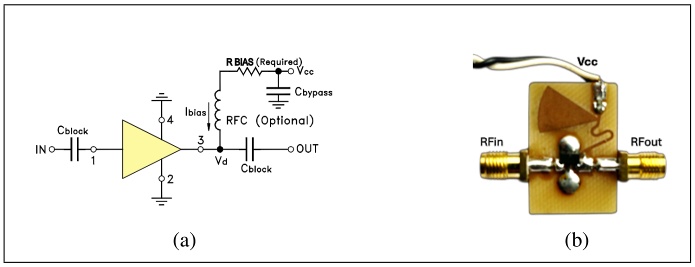

Fig. 6: the GALI-84+ power amplifier

In addition to the power amplifier, a 3 dB/90° Hybrid Coupler is used, functioning together as a duplexer to improve signal routing and isolation.

B. The 3 dB/90° Hybrid Coupler

In RF systems, duplexer are key components that allow signals to flow in one direction between ports, improving isolation and preventing signal reflection [4]. Instead of using a traditional duplexer, we implement a 3 dB 90° hybrid coupler to perform a similar function [18], [19]. This coupler acts like a circulator by routing signals efficiently between the PA,the LPDA and the receiver, helping to reduce interference and improve overall system performance.

The coupler has four ports with specific functions and connections, as shown in Fig. 7:

- **Port 1**: Input port of the coupler, connected to the power amplifier(PA) output.
- **Port 2**: Output port used for reception.
- **Port 3**: Output port connected to the antenna.
- **Port 4**: Isolated port terminated with a 50 Ω matched load to ensure proper isolation.

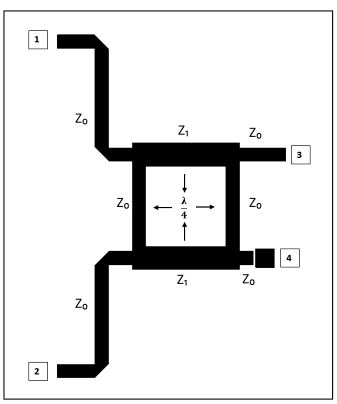

Fig. 7: Design of 3 dB/90° coupler

The structure of the coupler is based on quarter-wavelength transmission lines. According to the configuration shown in Fig. 7, the horizontal series branches are designed with a characteristic impedance $Z_1 = Z_0\sqrt{2}$, while the vertical shunt branches exhibit a characteristic impedance $Z_0 = 50\ \Omega$. All transmission line are implemented with an electrical length of $\lambda/4$ at the 2.4 GHz center frequency.

IV. MEASURED RESULTS AND DISCUSSIONS

To validate the proposed design and the conducted investigation, the fabricated LPDA antenna, with the connector soldered near to the shortest radiating element, was experimentally characterized. The reflection coefficient remains below -15 dB over the operating band (2.3–2.5 GHz), as illustrated in Fig. 8, which confirms good impedance matching.

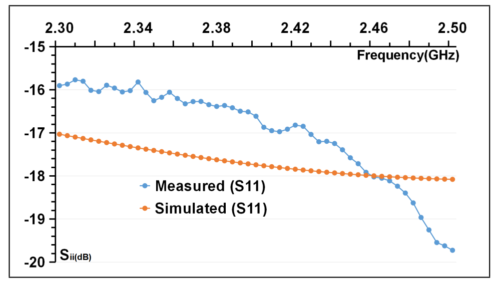

Fig. 8: Measurement vs simulated results of the simple antenna

Finally, to verify the impedance matching of the antenna, the complete system (antenna and feed line) is tested. The results shown in Fig. 9 indicate that the feed line effectively excites the antenna, with the reflection coefficient S_{11} remaining below -10 dB. This behavior confirms good impedance matching over the intended bandwidth.

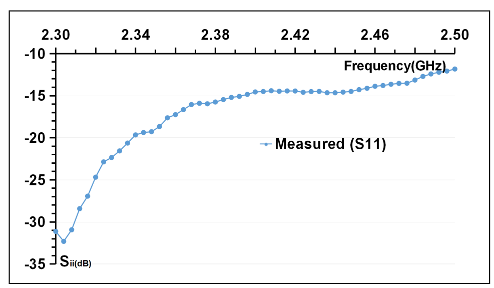

Fig. 9: Measurement results of the Antenna with Integrated Feed Line

The measured S-parameters of the amplifier shown in Fig. 10 provide insight into its matching and transmission performance. The input and output reflection coefficients, S_{11} and S_{22}, remain below -14 dB over the operating frequency range, indicating good impedance matching at both ports. The forward transmission coefficient, S_{21}, exhibits a gain of approximately $+17$ dB, confirming the proper amplification behavior of the circuit. In contrast, the reverse transmission coefficient, S_{12}, stays below -24 dB, demonstrating good reverse isolation and ensuring stable amplifier operation with minimal feedback.

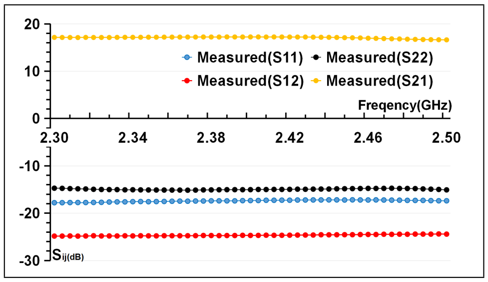

Fig. 10: Measurement results of the PA *S_parameter*.

The performance of the coupler is evaluated through the analysis of its S-parameters. In particular, the phase difference between the input and output ports is examined, as illustrated in Fig. 11. The impedance matching at the input and output ports is assessed using the reflection coefficients S_{ii}, shown in Fig. 12, while the power transmission between ports is characterized by the parameters S_{ij}, as presented in Fig. 12. Together, these results provide insight into the impedance matching, power balance, and isolation of the coupler, confirming its proper operation over the targeted frequency band.

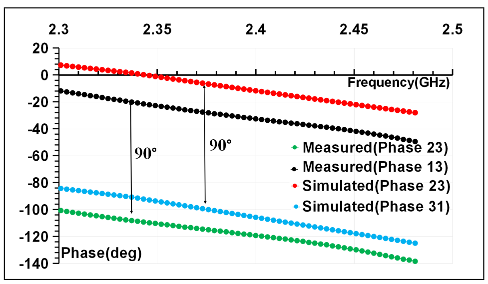

Fig. 11: Measurement vs simulation of the phase between ports of the coupler.

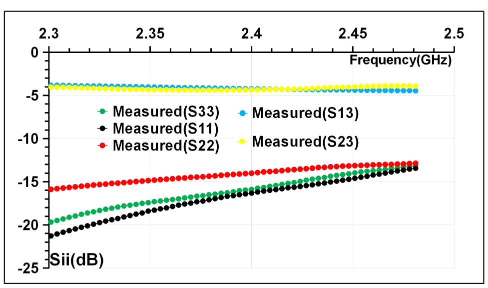

Fig. 12: Measured *S_parameter* of the coupler.

To create an active LPDA setup with a duplexer, we integrated a compact RF amplification stage based on the Mini-Circuits GALI-84+ MMIC at the coupler's input, as shown in Fig. 13. This active stage amplifies the signal directly at the feed point, reducing losses and improving the overall system sensitivity. The GALI-84+ offers wideband operation, stable gain and low noise, making it ideal for various applications.

In our design, the 3 dB/90° hybrid coupler acts as a duplexer: it directs the amplified signal to the LPDA for transmission, while during reception, the signal captured by the LPDA is routed to the receiver. Any signal traveling in the opposite direction is blocked from returning to the power amplifier, ensuring proper isolation and preventing interference.

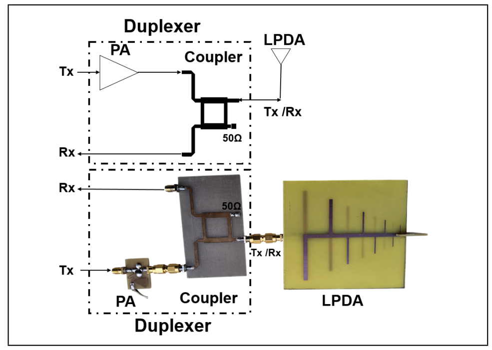

Fig. 13: Active LPDA with duplexer

Fig. 14 presents the reflection coefficients of the three duplexer ports. Both the input and output ports show good matching, with S_{11} and S_{22} remaining below about -14 dB across the frequency range of interest. In addition, the isolated port exhibits a pronounced minimum, with S_{33} dropping below -30 dB near the center frequency, which indicates that the coupled power is properly absorbed. Overall, these results demonstrate stable duplexer operation with low reflections and preserved isolation performance.

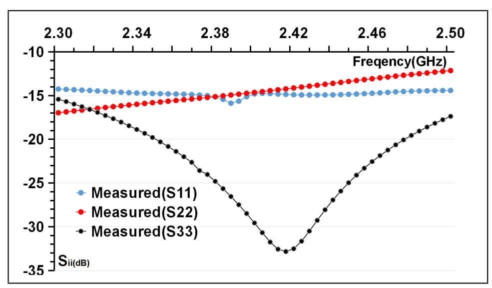

Fig. 14: Measured reflection coefficients of the duplexer ports

Fig. 15 shows the measured transmission and isolation responses of the duplexer formed by the hybrid coupler and the amplifier. The intended transmission path is clearly observed through S_{31}, which stays around $+10$ dB over the operating band, indicating that the signal is efficiently transferred and amplified in the desired direction. At the same time, the unwanted signal paths, represented by S_{12}, S_{13}, and S_{23}, are strongly attenuated and remain below -30 dB. This confirms that the duplexer provides effective isolation between the ports and limits any leakage between the transmit and receive channels.

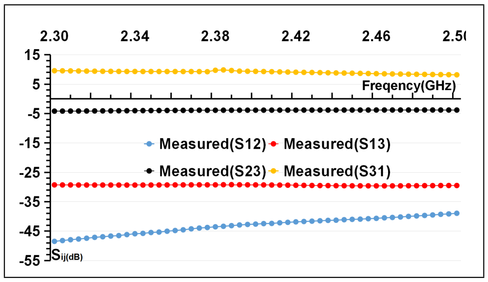

Fig. 15: Transmission and isolation responses of the proposed duplexer

V. Conclusions

In this paper, we introduced a simple design for an 8 element log periodic dipole antenna (LPDA) covering the 2.3–2.5 GHz frequency range. We proposed a new, cost-effective feed line that simplifies the traditional feeding setup. An amplifier was integrated at the input of the coupler, which serves as a duplexer in our system, to increase signal strength and reduce losses in the feeding network. The built prototype demonstrated stable performance with good impedance matching across the operating band, ensuring effective signal transfer. The strong correlation between simulations and measurements confirms the reliability of our design and manufacturing process. Overall, the results show that this antenna is a compact and broadband option suitable for wireless applications demanding enhanced signal quality. Future work may focus on antenna arrays and improving performance in complex multipath scenarios.

Abbreviations and Acronyms

- RADAR : Radio Detection And Ranging
- LPDA: Log-Periodic Dipole Antenna
- S-parameter: Scattering parameter
- RF: Radio Frequency
- PA: Power Amplifier

ACKNOWLEDGMENT

The authors thank the Sys'Com Research Laboratory, National Engineering School of Tunis (ENIT), University of Tunis El Manar, Tunis, Tunisia, for providing access to the equipment used in this study.

Special Thanks: The authors would like to express their sincere gratitude to the General Director of Military Research Center **Dr. Eng. Ahmed SIALA** for his invaluable support during the development of this work. His assistance in providing both human and material resources was crucial for the successful completion of this work.

References

[1] H. Wang and I. Park, "Compact Wideband Circularly Polarized Dipole Antenna Using Modified Quadrature Hybrid Couplers," *IEEE Transactions on Antennas and Propagation*, vol. 69, no. 12, pp. 8896–8901, 2021.
DOI: https://doi.org/10.1109/TAP.2021.3096321

[2] S. Velicheti and P. Mallikarjuna Rao, "An Analytical Review on Log Periodic Dipole Antennas with Different Shapes of Dipole Elements," *Lecture Notes in Electrical Engineering*, vol. 655, pp. 621–631, 2021.
DOI: https://doi.org/10.1007/978-981-15-3828-5_64

[3] F. Du and L. Jin, "Research on Miniaturization of Log-periodic Dipole Arrays Using Folded Dipole," *IOP Conference Series: Earth and Environmental Science*, vol. 170, no. 4, 2018.
DOI: https://doi.org/10.1088/1755-1315/170/4/042116

[4] Y. Barnadi, M. R. Istambul, K. S. A. Mayang, and S. Galih, "Isolation optimization method on the coupler," *Universal Journal of Electrical and Electronic Engineering*, vol. 6, no. 2, pp. 46–52, 2019.
DOI: https://doi.org/10.13189/ujeee.2019.061308

[5] K. Mistry, P. Lazaridis, I. Glover, V. Holmes, F. Khan, Q. Ahmed, Z. Zaharis, and T. Xenos, "Measurement, simulation and optimization of wideband log-periodic antennas," in *Proc. 32nd General Assembly and Scientific Symposium of the International Union of Radio Science (URSI GASS)*, pp. 1–4, 2017.
DOI: https://doi.org/10.23919/URSIGASS.2017.8105240

[6] B. A. M. P. C. Dharmarathna, H. D. T. S. Madusanka, and M. A. A. Karunarathna, "PCB Base Log-periodic Antenna for Mobile Communications," *Instrumentation*, vol. 8, no. 3, pp. 46–51, 2021.
Available: https://www.scopus.com/inward/record.uri?eid=2-s2.0-85203330591

[7] S. M. Hamza, H. Ullah, and F. A. Tahir, "A Miniaturized Printed UWB LPDA Antenna," in *Proc. 2020 International Conference on UK-China Emerging Technologies (UCET)*, pp. 1–3, 2020.
DOI: https://doi.org/10.1109/UCET51115.2020.9205322

[8] D. E. Isbell, "Log-periodic dipole arrays," *IRE Transactions on Antennas and Propagation*, vol. 8, pp. 260–267, 1960.
DOI: https://doi.org/10.1109/TAP.1960.1144848

[9] R. H. DuHamel and D. E. Isbell, "Broadband logarithmically periodic antenna structures," in *IRE International Convention Record*, vol. 9, pp. 119–128, 1961.
DOI: https://doi.org/10.1109/IRECON.1957.1150566

[10] R. H. Carrel, "Analysis and design of the log-periodic dipole antenna," PhD thesis, University of Illinois, 1961.
Available: https://catalog.hathitrust.org/Record/100697377

[11] A. A. Abdulhameed and Z. Kubík, "Review of Printed Log-Periodic Dipole Array Antenna Design for EMC Applications," *Inventions*, vol. 10, no. 3, Art. no. 34, 2025.
DOI: https://doi.org/10.3390/inventions10030034

[12] P. Rajput, P. Wankhade, and S. Gupta, "A Review on UWB Microstrip Patched Log-Periodic Antenna," *International Journal of Latest Trends in Engineering and Technology (IJLTET)*, vol. 7, no. 2, pp. 365–370, Jul. 2016.
DOI: http://dx.doi.org/10.21172/1.72.558

[13] F. Mejri and T. Aguili, "Design of a Microwave Duplexer without Ferrite and without Magnet," *Radioengineering*, vol. 27, pp. 494–500, Jun. 2018.
DOI: https://doi.org/10.13164/re.2018.0494

[14] L. F. Marzall, M. Pinto, A. Ashley, D. Psychogiou, and Z. Popović, "Co-simulations of DC magnetic bias fields and RF performance for microwave ferrite circulators," in *Proc. 2018 International Applied Computational Electromagnetics Society Symposium (ACES)*, pp. 1–2, 2018.
DOI: https://doi.org/10.23919/ROPACES.2018.8364098

[15] M. N. Zahid, F. Javeed, and G. Zhu, "Design analysis of advanced power amplifiers for 5G wireless applications: a survey," *Analog Integrated Circuits and Signal Processing*, vol. 118, no. 2, pp. 199–217, 2024.
DOI: https://doi.org/10.1007/s10470-023-02193-5

[16] Mini-Circuits, "GALI-84+ MMIC Wideband Amplifier Datasheet," Mini-Circuits, 2021. [Online]. Available: https://www.minicircuits.com/pdfs/Gali-84+.pdf.

[17] Y. Noh, D. Kim, S. Chang, H. Jung, and J. Lim, "X-Band GaN Power Amplifier MMIC Design and Radiation Evaluations for Space Applications," in *Proc. 2024 IEEE International Conference on Consumer Electronics-Asia (ICCE-Asia)*, 2024.
DOI: https://doi.org/10.1109/ICCE-Asia63397.2024.10773715

[18] J. B. Du Toit and J. Joubert and J. W. Odendaal, "Improved implementation of wideband 90° hybrids," in *Proc. of the 2022 International Conference on Electromagnetics in Advanced Applications (ICEAA)*,2022.
DOI:https://doi.org/10.1109/ICEAA49419.2022.9899897

[19] S. Qayyum and M.-D. Wei and R. Negra, "Wideband ring-hybrid with quadrature-phase outputs for high-power applications," in *Proc. of the 2015 German Microwave Conference (GeMiC)*,2015. DOI: https://doi.org/10.1109/GEMIC.2015.7107757